

# THE ROLE OF RESIDUAL THERMAL STRESS IN COMPOSITE INTERFACIAL STRENGTH BY A NOVEL SINGLE FIBRE TECHNIQUE

L. Yang<sup>\*</sup>, J. Thomason

*Department of Mechanical and Aerospace Engineering, University of Strathclyde, The University Centre, 347 Cathedral Street, Glasgow, G1 2TB*

*[\\*l.yang@strath.ac.uk](mailto:l.yang@strath.ac.uk)*

**Keywords:** Interfacial strength, Residual thermal stress, Microbond technique

## **Abstract**

*The temperature dependence of the interfacial properties of glass fibre reinforced polypropylene and epoxy composites was investigated using a novel microbond test in the temperature controlled environment of a thermo-mechanical analyser. Highly significant inverse dependence of IFSS on testing temperature was observed in both systems. The temperature dependence of the GF-PP IFSS was accounted for by the variation of residual radial compressive stresses at the interface with the test temperature. On the other hand, it was found that the residual thermal stress did not seem to fully account for the temperature dependence of IFSS in GF-Epoxy. Nevertheless, the results clearly showed that GF-Epoxy IFSS had a strong correlation with the modulus of the epoxy matrix.*

## **1 Introduction**

It is known that the properties of fibre reinforced polymer composites result from a combination of the fibre and matrix properties and the ability to transfer stresses across the fibre–matrix interface. Optimization of the stress transfer capability of the interfacial region is critical to achieving the desired mechanical performance in composites. The ability to transfer stress across the interface in composites is often reduced to a discussion of ‘adhesion’ which is a simple term to describe a combination of complex phenomena on which there is still significant debate as to what it means and how to measure it. Certainly, one of the generally accepted manifestations of ‘adhesion’ is in the mechanically measured value of interfacial shear strength (IFSS). Despite the high level of attention commonly focused on the chemical influences, such as silane coupling agents, on the level of IFSS in composites, a number of authors have commented on the role of shrinkage stresses contributing to the stress transfer capability at the fibre-matrix interface [1,2]. Most composite materials are shaped at elevated temperature and then cooled. Since in most cases the thermal expansion coefficients of polymers are much greater than that of the reinforcement fibres this cooling process results in compressive radial stress ( $\sigma_r$ ) at the interface [2,3]. Assuming that the coefficient of friction ( $\mu_s$ ) at the interface is non-zero these compressive stresses will contribute a frictional component  $\tau_{fs} = \sigma_r \cdot \mu$  to the apparent shear strength of the interface. In the case of thermoplastic polymer matrices where there may often be little or no chemical bonding across the interface these frictional stresses can make up a large fraction of the apparent IFSS [4].

Although it is unlikely that these residual stresses provide a full explanation of the IFSS in all composite systems, the above results do underline the need to better understand the role of fibre structure, the levels of residual stress, and the interfacial friction, on the IFSS in polymer composites. Most of the available models [2,3] of these phenomena indicate that the level of residual compressive stress at the composite interface should be directly proportional to the difference between matrix solidification temperature and the composite operating or test temperature ( $\Delta T$ ). Consequently, this would imply that the IFSS in polymer composites should also be dependent on  $\Delta T$ . In order to explore this concept an ability to accurately measure IFSS at different temperatures is required. IFSS is commonly measured using micromechanical test methods such as the fibre fragmentation test, the single fibre pullout test and the single fibre microbond test. Although these micromechanical test methods are commonly employed there is little, if any, standardisation of the testing apparatus. Furthermore, it is certainly the case that accurate control of the temperature of the test sample presents considerable challenges in the building of such micromechanical testing equipment.

Previously we have developed a method, which allowed us to measure IFSS of the composites at a wide temperature range [4]. In this paper we present data on the IFSS in a glass fibre-polypropylene and glass fibre-epoxy systems, in the temperature range  $-40^{\circ}\text{C}$  to  $150^{\circ}\text{C}$ , obtained using the microbond test in the temperature controlled environment of a thermo-mechanical analyser.

## 2 Experimental

### 2.1 Materials

Boron free uncoated and  $\gamma$ -aminopropyltrimethoxysilane coated E-glass fibre (average diameter =  $17.5\mu\text{m}$ ) were supplied by Owens Corning - Vetrotex and commercial isotactic homopolymer polypropylene PP 579S with melt flow index =  $47\text{ g}/10\text{ min}$  at  $230^{\circ}\text{C}$  was supplied by SABIC-Europe. The epoxy was Araldite 506 (DGEBA) cured with a triethylenetetramine (TETA), both supplied by Sigma-Aldrich UK.

### 2.2 Sample preparation

It has recently been reported that PP microdroplets for the microbond test should be formed in an inert atmosphere [5] to avoid thermo-oxidative degradation of the PP. However, this led to a very low yield rate for the axisymmetric droplets with respect to the fibre. This problem was solved by having the polymer surround the glass fibre prior to melting. A different method was used to form the microbond samples with epoxy. The resin and hardener were thoroughly mixed in stoichiometric proportions recommended by the manufacturer and degassed under a vacuum for 12 minutes. Epoxy droplets were then deposited on a single fibre using a thin wire, which had a small resin bead on its tip. Approximately 40 droplets were placed on the fibres before these samples were transferred into a convection oven, where they were heated first up to  $60^{\circ}\text{C}$  and held isothermally for 1 hour followed by another 2 hours heating at  $120^{\circ}\text{C}$ . The heating rate was set to be  $2^{\circ}\text{C}/\text{min}$ . After heating, the samples were left in the oven to cool down. The full cure was examined using a DSC, which indicated that there was no exothermic event in a temperature range from  $20^{\circ}\text{C}$  up to  $200^{\circ}\text{C}$  for the cured epoxy. The microbond samples of both GF-PP and GF-Epoxy were examined under a microscope prior to testing and the fibre diameter ( $D_f$ ), embedded fibre length ( $L_e$ ), and the maximum droplet diameter ( $D_m$ ) were measured under  $\times 200$  magnification.

### 2.3 TMA-Microbond

Development of the TMA-Microbond test (TMA-MBT) has been reported in [4] and will not be repeated here in detail. Figure 1 shows the experimental setup for the TMA-MBT. The droplet sits on a self-manufactured shearing plate, which rests on a stationary quartz probe. The movable probe, concentrically installed with the stationary probe, rests on the paper tab attached to the glass fibre as shown in Figure 1. The interfacial shear stress can be generated by pulling down the paper tab using the movable probe.

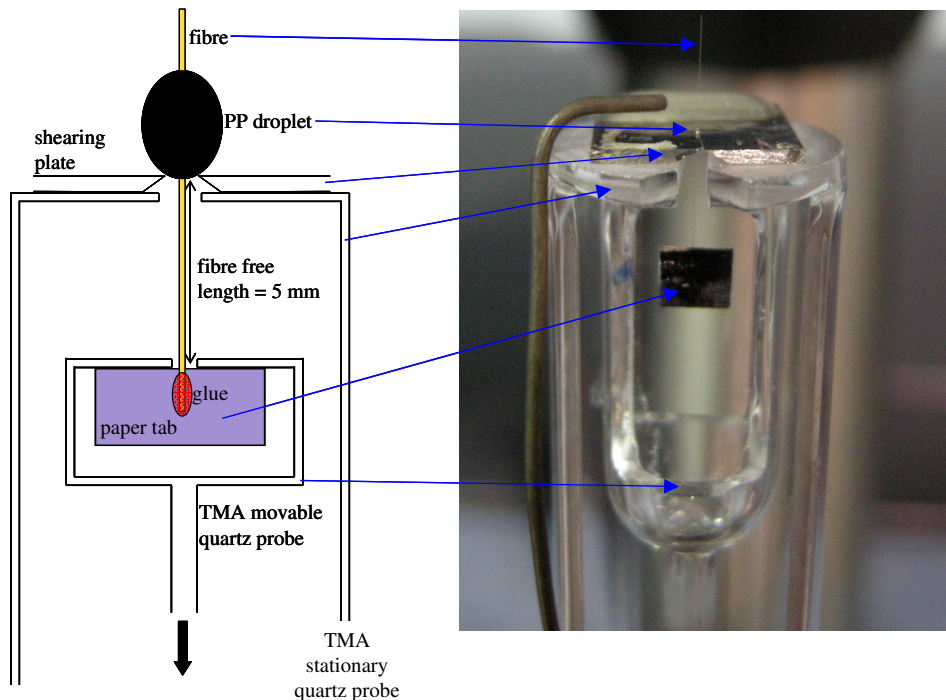


**Figure 1.** Schematic and close up photograph of the TMA-Microbond test configuration.

In this work, the measurement protocol proceeded as follows. The probe displacement was electronically zeroed and the single fibre microdroplet sample was loaded into the shearing plate with the lower paper tab hanging freely below the movable quartz probe. With the movable probe immobilised above the paper tab the furnace was closed. The initial sample length and probe position was recorded and then the furnace was equilibrated at the desired test temperature (in the  $-40^{\circ}\text{C}$  to  $150^{\circ}\text{C}$  range) with an additional 3-5 minutes isothermal segment to ensure a constant equilibrium temperature was attained. The movable quartz probe was then lowered very gently to contact the paper tab and the force ramp was initiated at  $0.15\text{ N/min}$ . The increasing probe displacement was then recorded until debonding occurred. A typical result obtained from a TMA-MBT is plotted as a Force-Displacement curve in Figure 2.

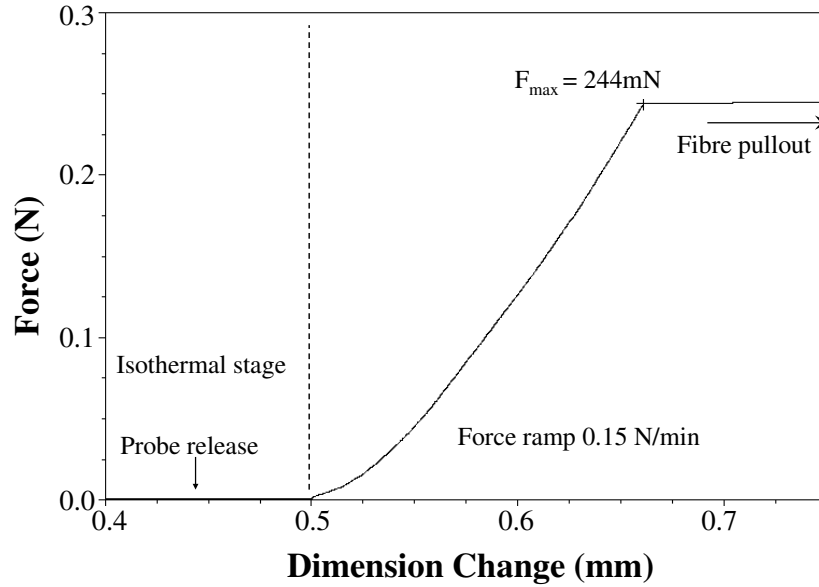


**Figure 2.** Load-Displacement curve from a typical TMA-Microbond test.

The general form of the curve is clearly different than that obtained in a “normal” force-displacement experiment. However, the maximum value of force ( $F_{\max}$ ) required to obtain a debonding event is still obtained. The major difference is what occurs after debonding. Since the TMA continues to attempt to increase the applied force above  $F_{\max}$  after debonding there is a rapid downward displacement of the debonded fibre. Consequently, in this test configuration, there can be no further information obtained on post-debond dynamic friction in a similar manner to the “normal” microbond test. The apparent IFSS ( $\tau_{\text{app}}$ ) was calculated by

$$\tau_{\text{app}} = \frac{F_{\max}}{\pi D_f L_e} \quad (1)$$

#### 2.4 Thermomechanical response of fibre and matrix

Characterisation of thermo-mechanical properties of PP and cured epoxy with dimensions 60x12.6x3.2 mm was carried in a DMA Q800 out by a three-point bending test with support span length of 50 mm and a heating rate 3°C/min from -60°C to 200°C, frequency 1 Hz, oscillating amplitude 100 µm (for PP) and 50 µm (for epoxy), static pre-load 0.1 N, and force track: 150%. The coefficient of linear thermal expansion (CLTE) of PP discs with dimensions of 6x1.6 mm and cured epoxy cube with dimensions of 3.5x3.5x4 mm was measured using a TMA Q400 with heating rate 3°C/min from -60°C to 200°C with a 0.1 N static force. Axial CLTE of 20 mm lengths of single glass fibre was also determined using a Q400 TMA heated at 3°C/min from -60°C to 200°C under 50ml/min nitrogen. Crystallisation behaviour of PP films of diameter 5.5mm and thickness 0.22 mm weighing approximately 5–6 mg was measured by using a differential scanning calorimeter Q1000 cooling from 250°C to room temperature at 10°C/min.

### 3 Results and Discussion

#### 3.1 Temperature dependence of IFSS in GF-PP

The results for IFSS obtained for GF-PP at five different test temperatures in the range -40°C to 100°C are summarised in Figure 3 which shows the average values with 95% confidence limits (between 25-45 individual measurements per temperature) of apparent IFSS plotted versus the testing temperature.

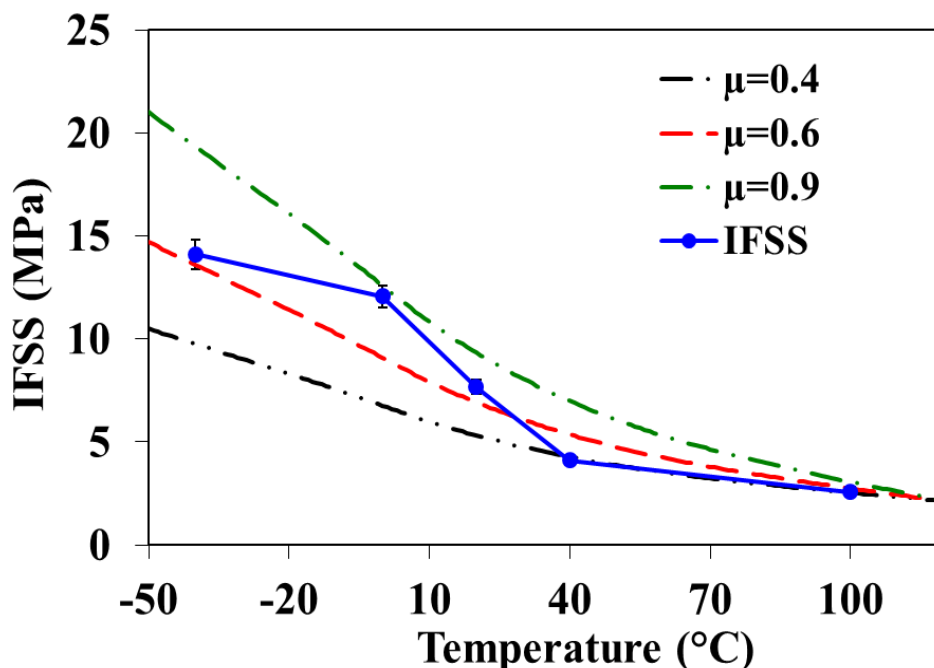


**Figure 3.** Comparison of average IFSS in GF-PP with residual frictional stress contribution calculated from IFSS concentric cylinder model with different values of static friction coefficient  $\mu$ .

It is clear from Figure 3 that the IFSS of GF-PP is significantly dependent on testing temperature. It is worth noting that the rate of change of IFSS with temperature is highest around room temperature (approximately 0.2 MPa/°C at 20°C) which is in the region of the glass transition temperature ( $T_g$ ) of the PP matrix ( $-10 < T_g < 10^\circ\text{C}$  depending on the preferred method for defining  $T_g$ ). It is well known that the scatter in the measurement of IFSS using the microbond test can often be quite high. The results in Figure 8 indicate that variations of the sample test temperature, for instance over the length of a day or more extremely summer to winter comparisons, could contribute significantly to observed scatter in the results for IFSS measured in polypropylene matrices.

As previously discussed an increase in IFSS with decreasing temperature is a phenomenon which would be expected if compressive residual stresses and interfacial static friction play a significant role in the interfacial stress transfer capability in this system. If the temperature dependence of the fibre and matrix modulus and expansion coefficients is known then the residual compressive stress ( $\sigma_r$ ) at the GF-PP interface can be calculated from available models [2,3]. We used the concentric cylinder model combined with the results from thermomechanical characterisation in section 2.4 to calculate  $\sigma_r$ . For bare GF-homopolymer PP we assumed there was no interphase between the fibre surface and the bulk matrix. The potential contribution to apparent IFSS of  $\sigma_r$  was calculated using various values of coefficient of static friction and added to the IFSS value ( $\tau_0$ ) extrapolated at the stress free temperature of 120°C in Figure 3. The combination of components based on residual stress

( $\sigma_r$ ) and physiochemical molecular interactions ( $\tau_0$ ) at the interface may then fully account for the measured IFSS on a basis of the coulomb friction law. For the sake of simplicity, we first assume that  $\tau_0$  is independent of temperature and  $\sigma_R$  enabling the measured IFSS value ( $\tau_{ult}$ ) to be modelled by

$$\tau_{ult}(T) = \tau_0 + \mu\sigma_r(T) \quad (2)$$

The experimental values for GF-PP IFSS at different temperatures are compared with values of ( $\tau_{ult}$ ) calculated using equation 2 and various values of  $\sigma_r$  in Figure 3. It can be seen that the residual interfacial stress builds up significantly as the temperature is lowered. Furthermore, the experimental IFSS data fall well within the range of values of interfacial shear strength contribution for coefficients of static friction between 0.4-0.9. There is very little information available on  $\mu$  in the literature, however Schoolenberg reported a value for  $\mu=0.65$  in a sized glass fibre-polypropylene system [6]. The glass fibre used in GF-PP was unsized and consequently there is some uncertainty as to the accuracy of using this value, however it does give the appropriate order of magnitude for  $\mu$  in GF-PP.

### 3.2 Temperature dependence of IFSS in GF-Epoxy

The results for IFSS obtained for GF-Epoxy at seven different test temperatures in the range 20°C to 150°C are summarised in Figure 4 which shows the average values with 95% confidence limits (between 10-20 individual measurements per temperature) of apparent IFSS plotted versus the testing temperature.

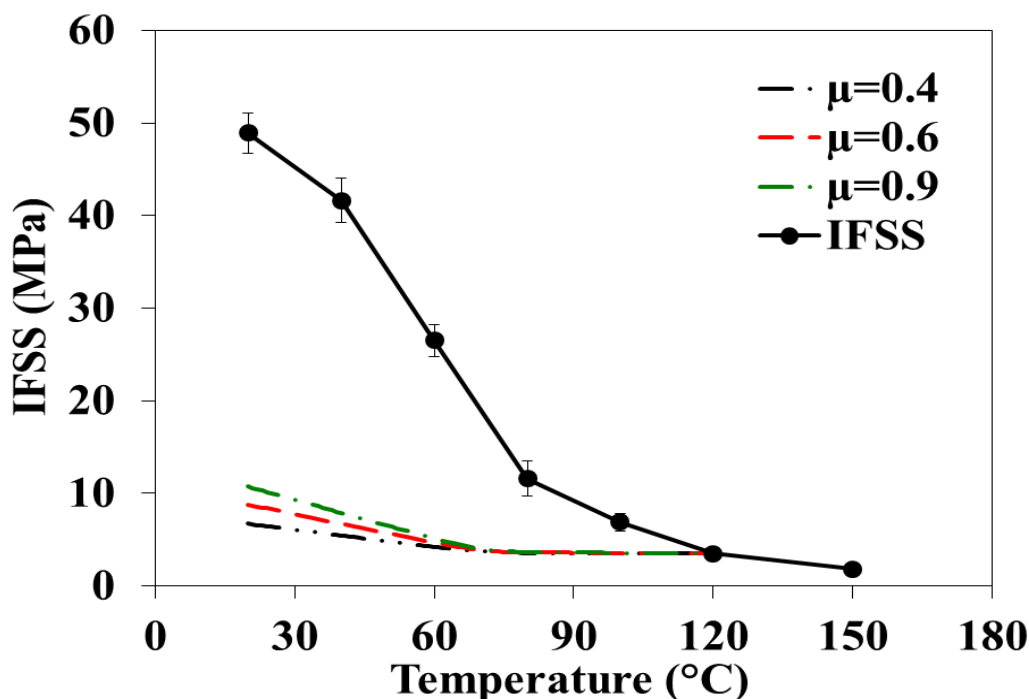


**Figure 4.** Comparison of average IFSS in GF-Epoxy with residual frictional stress contribution calculated from IFSS concentric cylinder model with different values of static friction coefficient  $\mu$ .

It can be clearly seen that there also exists a significant temperature dependence of measured IFSS in this thermosetting system. The IFSS drops from 49 MPa at 20°C to just 3.5 MPa at post-cure temperature, 120°C, which is assumed to be the stress free temperature. It is

noticeable that the highest rate of change of IFSS with temperature is also in the region of the glass transition temperature ( $T_g$ ) of the epoxy matrix ( $60^\circ\text{C} < T_g < 80^\circ\text{C}$  according to thermal analysis in section 2.3) with  $0.75\text{MPa}/^\circ\text{C}$  at  $60^\circ\text{C}$ . This value is almost 4 times higher than that in GF-PP at  $20^\circ\text{C}$ . The residual frictional stress contribution in GF-Epoxy was calculated using the same model as in GF-PP and the results are presented in Figure 4. The authors have not yet found any direct information on the coefficient of static friction,  $\mu$ , between the glass fibre and the epoxy. Bowden measured the IFSS in Steel wire-Epoxy using a typical fibre pull-out configuration under different hydrostatic pressures at the wire-matrix interface and 0.5 was obtained for  $\mu$  in that work [7]. At this stage we will assume the same level of  $\mu$  in GF-Epoxy as in GF-PP, although it may be reasonable to say that  $\mu$  should be higher for GF-Epoxy. With these low values of  $\mu$ , it is not surprising to see that the residual frictional stress appears to play an insignificant role in the GF-Epoxy IFSS compared to that in GF-PP. The results in Figure 4 also suggest that the IFSS in GF-Epoxy may not be mainly accounted for by the friction model as for GF-PP system. The IFSS in GF-Epoxy at the stress free temperature is found to be higher than that in GF-PP and it continues decreasing as the increase of the temperature afterwards.

Figure 5 shows the relation of both the IFSS and the storage modulus of the epoxy with the test temperature.

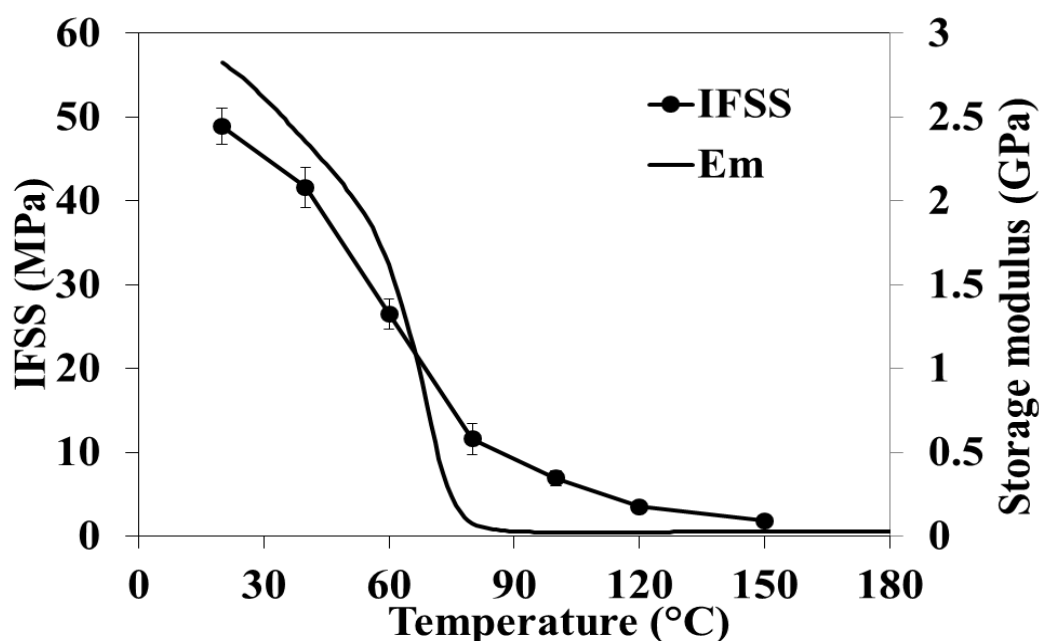


**Figure 5.** Comparison of temperature dependence of average IFSS in GF-Epoxy and storage modulus of epoxy matrix.

It can be seen that the temperature dependence of both parameters shares a rather similar trend. The strong temperature dependence of the IFSS in epoxy composites with other fibres has been reported in the literature and the highest rate of change of IFSS with temperature usually appeared around  $T_g$  as well [7].

#### 4 Conclusions

In order to investigate the temperature dependence of the interfacial properties of fibre reinforced composites the microbond test has been successfully adapted to be carried out in the temperature controlled environment of a thermo-mechanical analyser. This novel technique was applied to bare glass fibre-homopolymer polypropylene and APS sized glass fibre-epoxy respectively. Highly significant inverse dependence of IFSS on testing temperature was observed in both systems. This temperature dependence of the GF-PP IFSS was interpreted as being due to the increase in residual radial compressive stresses at the interface as the test temperature is lowered. The analysis indicated that approximately 70% of the value of the IFSS in this GF-PP system measured at room temperature could be attributed to residual radial compressive stresses at the interface. This would seem to be supportive of the hypothesis that the interface in this system is dominated by residual thermal stresses. On the other hand, it was found that the residual thermal stress did not seem to fully account for the temperature dependence of IFSS in GF-Epoxy. Nevertheless, the results clearly showed that GF-Epoxy IFSS had a strong correlation with the modulus of the epoxy matrix.

## 5 Acknowledgements

The authors would like to thank Owens Corning Vetrotex and SABIC-Europe for providing the materials used in this study.

## References

- [1] Nairn J.A., Zoller P. Matrix solidification and the resulting residual thermal stresses in composites. *Journal of Materials Science*, vol. **20**, pp. 355-367, (1985).
- [2] Nairn J.A., Thermoelastic analysis of residual stresses in unidirectional, high-performance composites. *Polymer Composites*, vol. **9**, pp. 123-130, (1985).
- [3] Wagner H., Nairn J.A. Residual thermal stresses in three concentric transversely isotropic cylinders: Application to thermoplastic-matrix composites containing a transcrystalline interphase. *Composites Science and Technology*, vol. **57**, pp. 1289-1302, (1997).
- [4] Yang L., Thomason J. Temperature dependence of the interfacial shear strength in glass fibre-polypropylene composites. *Composites Science and Technology*, vol. **71**, pp. 1600-1605, (2011).
- [5] Yang L., Thomason J. The influence of thermo-oxidative degradation on the measured interface strength of glass fibre-polypropylene. *Composites Part A: Applied Science and Manufacturing*, vol. **42**, pp. 1293-1300, (2011).
- [6] Schoolenberg G.E. Some wetting and adhesion phenomena in polypropylene composites in "Polypropylene: structure, blends and composites", edited by Karger-Kocsis J. Chapman and Hall, London, **3**, (1995).
- [7] Bowden P.B. The effect of hydrostatic pressure on fibre-matrix bond in a steel-resin model composite
- [8] Dibenedetto A.T., Lex P.J. Evaluation of surface treatments for glass fibres in composite materials. *Polymer Engineering and Science*, vol. **29**, pp. 543-555, (1989).